NMR of peptides

S. Raghothama

Abstract | Developments and applications of NMR spectroscopy especially with biomolecules has taken big strides over the decades. This review gives a brief overview of peptide analysis by NMR as carried out in the author's laboratory. A brief introduction to peptide biomolecules and NMR useful parameters are discussed in the beginning. This is followed by diagnostics features observed in NMR for identification of secondary structures. It further goes on to show how a three dimensional structure could be obtained by all-important NOE and hydrogen bond information. Use of heteronuclear experiments, which could be done at natural abundance is also highlighted in getting more details of peptide structures. Applications using Solid state NMR at natural abundance in connecting peptide solution and x-ray structures is demonstrated with couple of examples.

1. Introduction

Over the years, consistent developments in NMR spectroscopic techniques have led to large number of applications [1–3]. Limitations like low sensitivity, strong coupling effects, poor dispersion of signals is thing of the past due to availability of well-shielded, high field magnets. In addition, cryo probes boosted the sensitivity factors by orders of magnitude. RF electronics providing very fine phases and fast switching delays for the pulses make robust experimental setup providing variety of options and opening a wide angle in tackling a problem. Yet another dimension added is the ease of doing heteronuclear experiments even at natural abundance greatly assisted by polarization transfer experiments [4]. Future seems even more promising with recent developments in Dynamic Nuclear polarization (DNP) [5]. Current developments include reduction in experiment time by orders of magnitude in conducting multidimensional experiments by (i) single scan NMR spectroscopy [6], (ii) G-matrix Fourier transform NMR [7], (iii) Projection reconstruction technique [8], (iv) Automated projection spectroscopy (APSY) [9]. Development in solid state NMR has also claimed up. High magic angle spinning speed reaching 70–80 KHz , better decoupling / recoupling sequences has opened up a large window for biomolecular NMR [10]. Recording NMR spectra in micro-molar concentration is not difficult at all, but again doing multidimensional NMR of biologically important involving rare nuclei like ^{13}C and ^{15}N at natural abundance continues to be quite a challenge.

X-ray diffraction and NMR spectroscopy are the two main tools to get structural details at Molecular level. If single crystals could not be obtained, then NMR is the method of choice to probe the structural details. Otherwise also, used complimentarily, they add better clarity and understanding of structures. Influence of crystal packing may induce one of the possible structures especially in peptides where coexistence of multiple conformations is quite common [11,12]. NMR would be an ideal tool in such cases. Depending on the interconversion rate one gets multiple sets of resonances whose individual structures can be simultaneously derived using NMR parameters provided it is limited to a few, say around 2–4 conformers. Higher numbers lead to overlap of resonances making the analysis difficult. Another advantage in NMR in such cases is

NMR Research Centre, Indian Institute of Science, Bangalore 560012
sr@sif.iisc.ernet.in

the possibility of temperature variations, which can influence the conformation equilibrium depending on the energies involved.

Solid state NMR provides new avenues to further probe these investigations. The whole lot of information dominated by dipolar coupling, quadrapolar coupling, chemical shift anisotropy, etc. increases the complexity of the spectrum. But that is where a wealth of information is hidden which is lost in case of solutions due to Brownian motions. Again recent developments to remove and add these interactions selectively make it a treasure house to pull out the required information [13–16]. Some understanding of quantum mechanics would be very helpful to do the gymnastics of spin dynamics. Similar support from the software side aiding in number of efficient decoupling techniques which are very power efficient help in reduction in sample heating thus protecting biomolecule degradation. This way both homogeneous and heterogeneous interactions can be controlled to obtained the desired information on the molecules. Still the information on ^{1}H is limited especially due to strong homogenous interactions, which are very difficult to remove. However, it is possible to get some information on ^{1}H by heteronuclear experiements like ^{1}H–^{13}C HSQC even at natural abundance [17, 18]. Large amount of heteronuclear studies are available in literature but the problem still is the need of molecules with nmr active nuclei labeled such as ^{13}C and ^{15}N, when it comes to solid state NMR structure determination of biomolecules. Huge amount of structure data collected by NMR in the data bank is leading to structure information straight from the chemical shift itself [19–21]. This has given some impetus to study peptide conformations by solid state NMR at natural abundance.

This review mainly dwells on our own efforts using NMR for peptide conformation elucidation mainly by solution NMR followed by our initial attempts at solid state NMR main focused at natural abundance. We start with a very brief description of peptides and proteins.

Figure 1: Schematic representation of polypeptide chain. Partial double bond across peptide bond restrict the rotation (ω) around C′–N bond(carbonyl carbon is generally referred as C′). Peptide fold is defined by the remaining two backbone dihedral angles ϕ and ψ across N-C$^{\alpha}$ and C$^{\alpha}$–C′ bond respectively.

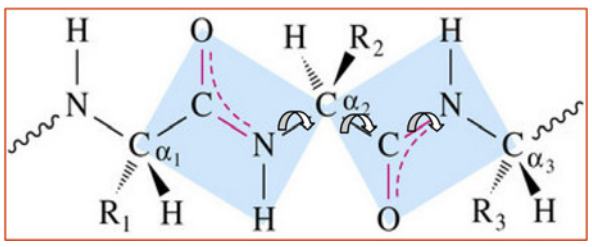

1.1. *Peptides and proteins*

Peptides are generally short linear chain of amino acids of varying length linked by peptide bonds. As the chain length increases they are called polypeptides. When sufficiently long they fold and when a function get associated with it they take the name Proteins [22,23]. The number of amino acids making such a protein can run into hundreds whose molecular weights can vary between a few Daltons to Kilo or Mega Daltons. It is very useful to know their three dimensional structure as they are related to its function. When it comes to structure determination, X-ray diffraction has no limitation on size as long as they are obtained in single crystal form. Whereas, in NMR the order of difficulty increases as size increases. But in this article we are restricting ourselves to peptide NMR.

1.2. *Protein fold and Ramachandran Map*

It is well known that three dimensional structure is largely defined by three backbone torsion angles ϕ, ψ and ω as shown in Figure 1. As the peptide bond has partial double bond character, rotation around C′–N bond defined by ω is restricted to 180° or trans geometry. Rarely in isolated cases, especially whenever a Proline residue is present, it can flip to cis form, ω gets restricted to 0°. Hence the key to polypeptide fold is mainly defined by free rotation around N–C$^{\alpha}$ and C$^{\alpha}$–C′ bonds represented by ϕ, ψ torsion angles respectively, as bond lengths and bond angles remain invariant. Though it is now reduced to two dimensional problem, still the canvas is too large as both ϕ and ψ individually can span a range of 0–360°. Considering an average protein containing 100 amino acids and at each residue, if the ϕ and ψ torsions are allowed to search and select from the canvas, the number of possible folds that can be generated and the time taken touches astronomical figures. But when these proteins come out of cell they come out having a particular fold within few seconds. This phenomenon is exemplied by the famous Lavinthal paradox [24–25].

Ramachandran in his pioneering work on ϕ vs ψ plot, famously known as Ramachandran map [26,27], showed that due to steric effects in poly peptide sequence, only a limited region of ϕ and ψ are allowed as shown for an L-residue (other than Proline and Glycine) (Figure 2.) which is only about one fourth of the whole map area. The regions corresponding to main secondary structures α-helix and β-sheet are identified on the map. It is embedded in structural biology now that any protein structure whichever way it is determined has to be validated by Ramachandran Map.

Figure 2: Ramachandran map connecting the ϕ and ψ torsion angles. Main secondary structure such as α-helix and β-sheet regions are identified.

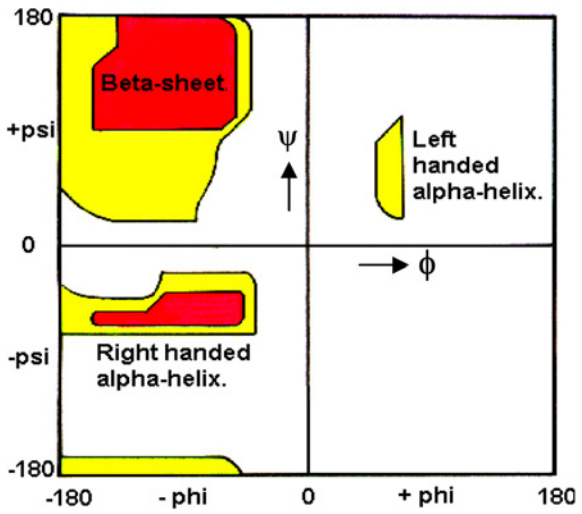

Figure 3: Schematic represenation of (a) chemical shift (δ) spread, (b) $^3J_{NHC^\alpha H}$ spin-spin coupling distribution in case of helices and β-sheet s. Inset shows the Karplus curve which is used to estimate the ϕ value from this J value.

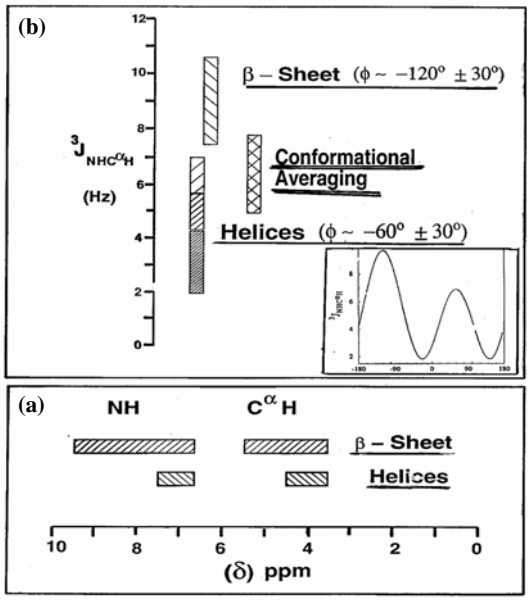

2. NMR parameters in diagnosis of secondary structures

The major parameters of NMR such as, Chemical shift, scalar spin-spin coupling and NOE all carry signatures of these secondary structures. The other parameters, relaxation rates T_1 and T_2 can provide more information as we go deeper into conformational aspects.

2.1. *Chemical shifts* (δ)

It is the most influenced parameter, which took NMR into the realm of chemistry. Each resonance in the NMR spectrum represent a unique nucleus influenced by its chemical environment. Further, peptide/protein secondary structures also show their influence on the chemical shifts. Hence from ^{1}H spectrum, secondary structures can be identified by shift patterns of amide and C$^\alpha$ proton resonances, which show distinct features in their chemical shifts.

Figure 3a shows a schematic depiction of these shifts. In case of extended conformation, the spectrum is well dispersed and many resonances would be downfield shifted. Whereas helical conformation show limited spread and upfield shift of resonances. Wishart and sykes [28–29] used this property and came out with chemical shift index (CSI) plot which can predict the stretches of secondary structures in a given protein sequence just from chemical shift information. They further showed similar information can also be obtained from ^{13}C chemical shifts as well. Yet another use of the ^{13}C chemical shift is the prediction of cis / trans isomers across Xxx-Pro bond. It has been shown that the chemical shift difference ($\Delta\delta$) between C$^\beta$ and C$^\gamma$ carbon of Proline residue, is larger ($\sim$ 10 ppm) in case of cis isomer, in contrast to $<$ 5 ppm in case of trans isomes [30–31].

An interesting example is shown in Figure 4. It illustrates amide and C$^\alpha$ proton region of ^{1}H spectra on two peptides, Boc-Leu-Val-Val-Ac$_6$c-^{D}val-Leu-Val-Val-OMe (1) and Boc-Leu-Val-Val-Ac$_6$c-^{L}val-Leu-Val-Val-OMe (2) that differ only in the configuration of fifth residue (^{D}Val to ^{L}Val). Peptide 1 with centre segment Ac$_6$c - ^{D}Val, takes up a β-hairpin conformation. The connecting two sheets, -(Leu-Val-Val)- segment on either side show large chemical shift dispersion and many of its resonances are relatively downfield shifted. In comparison, peptide 2, which differs only in the fifth residue configuration (^{D}val to ^{L}Val) takes up helical conformation throughout the sequence. Here the amide and C$^\alpha$ protons have limited chemical shift dispersion and relatively upfield shifted, clearly demonstrating influence of secondary structure.

2.2. *Spin-spin coupling*

During initial developments of NMR itself Karplus [32] showed correlation between scalar spin-spin coupling and dihedral angles in many chemical compounds. It turned out to be very useful in

Figure 4: Partical 1D spectra from peptide (1) Boc-Leu-Val-Val-Ac_6c-^{D} Val-Leu-Val-Val-OMe and Boc-Leu-Val-Val-Ac_6c-^{L} Val-Leu-Val-Val-OMe showing amide and c^{α} proton region. Extended conformation in (1) results in larger dispersion of chemical shifts.

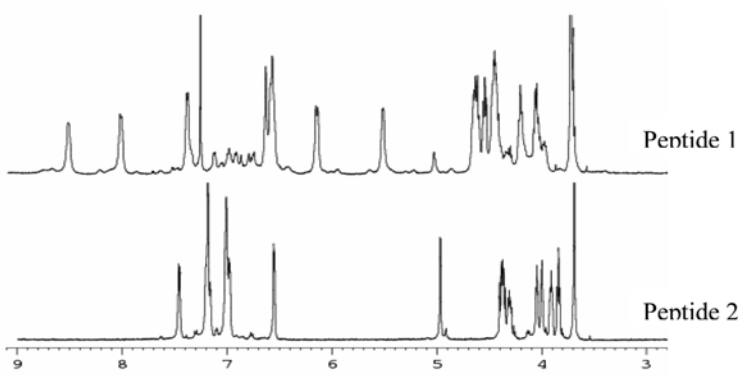

predicting peptide secondary structures [33, 34]. To put it in simple terms, the dihedral angle ϕ is related to $^{3}J_{NHC^{\alpha}H}$ through the Karplus curve shown in the inset of figure 3. A small $^{3}J_{NHC^{\alpha}H}$ value less than 4 Hz indicate a ϕ value nearing $\pm 60°$ typical of helices and a value greater than 8 Hz would be typical of extended stretch where ϕ would take up value around $\pm 120°$. Hence a $^{3}J_{NHC^{\alpha}H}$ around 6–7 Hz would reflect random coil dihedral angles. Similarly, the other dihedral angles ψ, and χ can also be estimated from other homo- and hetero-nuclear spin-spin couplings [33].

Figure 5: Plot of NOE/ROE intensity (η) vs τ_c at different spectrometer frequencies.

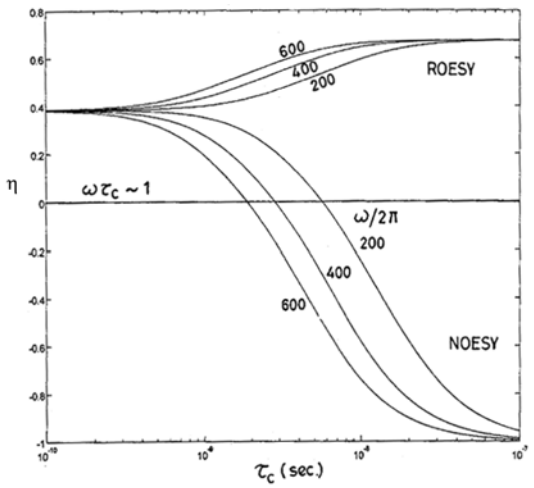

2.3. *Nuclear Overhauser Effect (NOE)*

Currently this is the most useful NMR parameter for obtaining 3-dimentional or tertiary structure. It is a through space interaction mediated mainly by dipolar interaction [35,36]. It is defined as change in integral intensity of a particular resonance when another resonance is saturated. A two dimensional NOE, called NOESY [37,38], provide all NOE correlations in one single 2D map. NOE is expressed as percentage change, which is related to internuclear distances. It is also a function of $\omega\tau_c$ where ω is the spectrometer frequency and τ_c is rotation correlation time of the molecule. This relation is expressed as:

$$\mathrm{NOE} = (1/r^{6}) \times f(\tau_c) \qquad (1)$$

Figure 5 shows plot of NOE / ROE intensity (η) vs τ_c at different spectrometer frequencies (ω). As molecular size increases (and hence increase in rotation correlation time (τ_c)), the NOE enhancement decreases. It crosses zero at $\omega\tau_c \sim 1.1$ and later becomes negative. The ROE curve remains always positive for all values of $\omega\tau_c$. It is a big concern for peptide molecules with molecular weight around 1 to 2 KD which fall in this $\omega\tau_c \sim 1.1$ region. There is very little or no NOE enhancement around this region. A simple way to overcome this problem is to consider ROE enhancement. It is nothing but NOE in rotating frame, whose 2D version is called the ROESY [39,40]. The added advantage in ROESY is easy distinction of exchange cross peaks. Exchange cross peaks are common in peptides as they often undergo conformation exchange. ROE cross peaks are always positive [41], whereas the exchange peaks would be negative

Table 1: Comparative table between NOESY vs ROESY.

Sl. No.	Parameter	NOESY	ROESY
1.	Magnetization transfer	Longitudinal axis	Transverse axis
2.	NOE Intensity	$+0.38$ to -1.00	$+0.38$ to $+0.68$
3.	Cross peak buildup rate	Slow	Fast (double)
4.	Usefulness: small molecules ($\omega\tau_c \ll 1$) Intermediate size ($\omega\tau_c \sim 1$) macro molecules ($\omega\tau_c \gg 1$	 Useful. Buildup rate is slow Not useful, zero NOE Preferred, Good NOEs	 Useful: buildup rate is fast Preferred, ROE is always +ve, Can be used with caution
5.	Chemical exchage	Difficult to identify – diagonal and cross peaks – same sign	Easy identification – Diagonal and cross peaks – opposite sign
6.	Spin diffusion	High probability	Very low probability – hence useful
7.	Artifacts	Minimal (big advantage)	Problem (Probable TOCSY and offset effects)

Figure 6: Schematic representation of amide protons in peptide structures. (a) A typical hydrogen bonded amide proton shown as shielded and the other as exposed. (b) In non-hydrogen bonding solvents like $CDCl_3$ the solvent just surround the solute molecules without any interaction. (c) Hydrogen bonding solvents like DMSO.d_6 form intermolecular hydrogen bond with the exposed amide protons. (d) Plot of chemical shift vs percentage addition of DMSO.d_6 for the two type of amide protons which is either shielded or exposed.

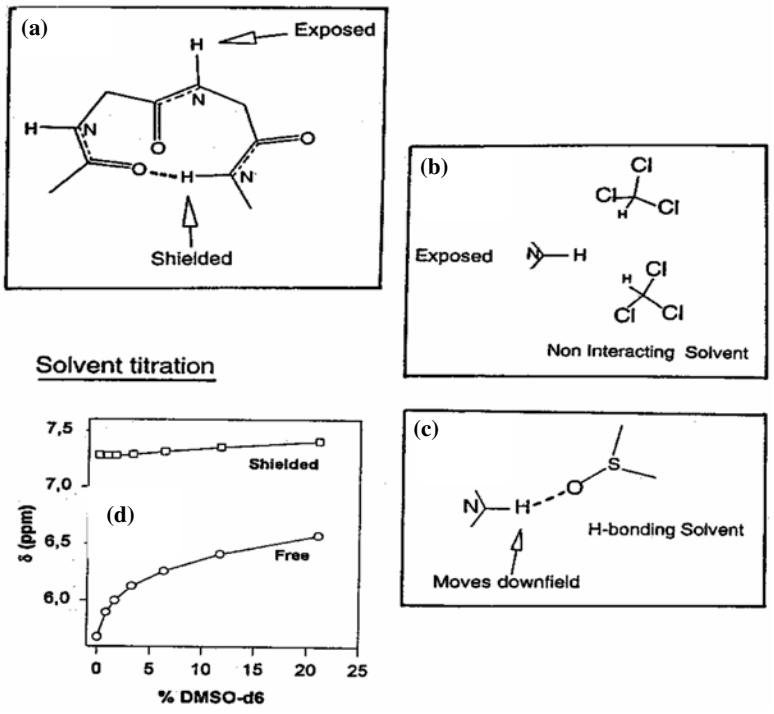

and hence the easy distinction. The ROESY pulse sequence has a spin lock pulse, which holds the magnetization in the transverse plane by a train of rf pluses. This creates a situation where the spins only see the RF magnetic field, which are orders of magnitude less than the main static magnetic field. Essentially this makes $\omega\tau_c \ll 1$ and hence the so called ROE will always be positive for the entire range of τ_c under consideration, as shown in figure 5. Though this comes as a big relief of peptide structure analysis by NMR, care has to be taken with ROESY experiments, as it is highly susceptible for

artifacts, hence better used only in case of necessity. Yet another advantage of ROESY is in overcoming spin diffusion problem. The cross peak buildup rates are doubled in ROESY when compared with NOESY. Table. 1 lists out the differences between NOESY and ROESY which may be helpful in case of doubt in deciding which is more suitable for a given molecule.

There are diagnostic NOEs to distinguish helical and extended secondary structures. A continuous stretch of strong sequential $N_iH \leftrightarrow N_{i+1}H$ represented as $d_{NN(i,i+1)}$ NOE is very characteristic of helical structure. Similarly a strong sequential $C^{\alpha}_{i}H \leftrightarrow N_{i+1}H$ represented as $d_{\alpha N(i,i+1)}$ NOEs indicate extended stretch.

3. Hydrogen bond

It is one of the major interactions contributing to stabilization of secondary structures in peptides and proteins. Delineation of Hydrogen bonds play an important role in peptide conformations especially with secondary structures like helices and β-sheets. Typical α-helicx is identified by sequential $5 \rightarrow 1$ $(i, i+4, 13$ atoms) hydrogen bond. That is to say ith residue carbonyl oxygen is hydrogen bonded to $(i+4)$th amide proton. Such a hydrogen bond would have 13 backbone atoms between them. Similarly a 3_{10} helix would have $4 \rightarrow 1$ $(i, i+3, 10$ atoms) hydrogen bond. In such helices, the first 3 or 2 N-terminus residues would have amide hydrogen exposed or so to say not hydrogen bonded. Similarly β-sheets are also stabilized by hydrogen bonds across the strands. It is possible in NMR to identify such hydrogen bond characteristics.

3.1. *Amide Hydrogen bond*

Detection of amide protons involved in hydrogen bond or otherwise, are quite straightforward in NMR. But to which carbonyl oxygen or other acceptor it is hydrogen bonded to is difficult to infer. Electron withdrawing nature of the acceptor group makes the involved amide proton chemical shift to be downfield shifted. This shift can be monitored in various ways as described below to identify exposed or hydrogen bonded nature of amide protons in peptide sequences.

3.1.1. *Solvent titration*

Figure 6, shows a schematic diagram of a typical peptide turn where one of the amide proton

Figure 7: (a) Intermolecular hydrogen bond breaks upon heating, resulting in (b) upfield shift of the associated amide proton.

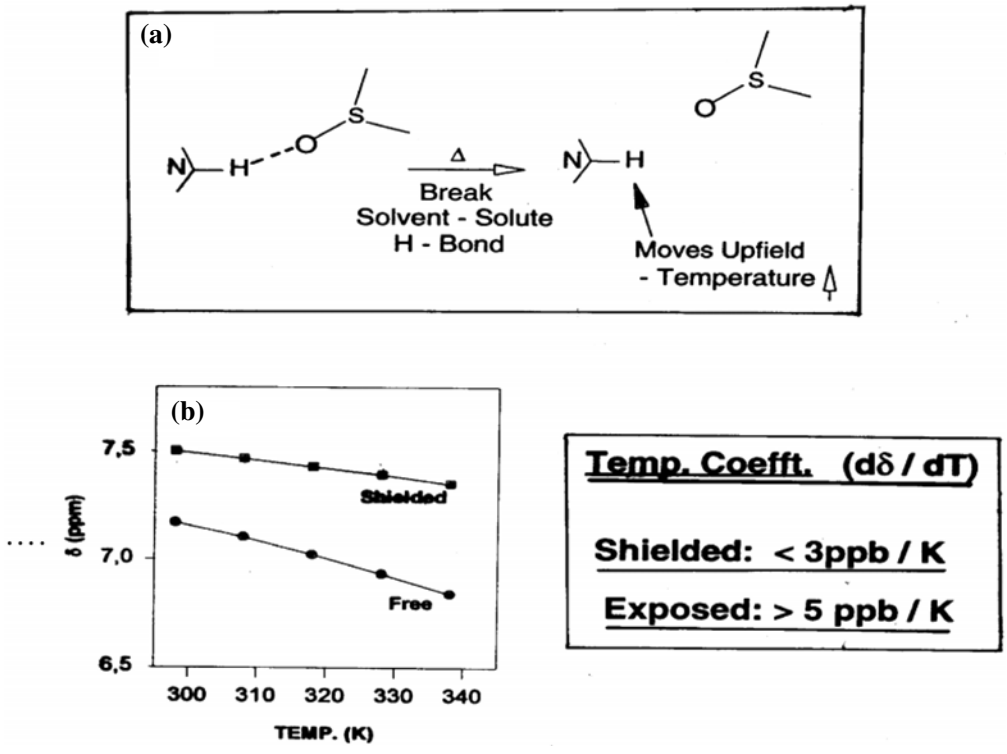

Figure 8: Amide proton/Deuterium exchange. (a) A schematic representation. (b) Plot of 500 MHz amide region of a 19 residue peptide as a function of time after addition of CD_3OD. Some of amide resonance still remain as they do not exchange even after 80 hours indicating strong hydrogen bonded nature for these amide protons.

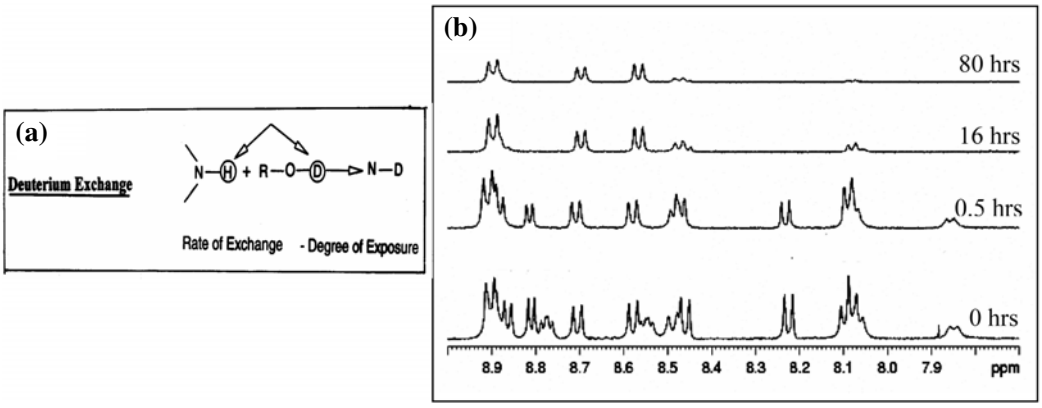

is hydrogen bonded and the other is exposed. The commonly used $CDCl_3$solvent molecules simply surround the solute molecules without any interaction. While titrating with hydrogen bonding solvents like DMSO.d_6, the exposed amide proton from the solute molecule form intermolecular hydrogen bond with the –SO group of the solvent. This results in downfield chemical shift of the involved amide proton. A plot of chemical shift vs percentage addition of DMSO.d_6 clearly distinguish the intermolecular hydrogen bonding amide proton from the already intramolecularly hydrogen bonded or shielded amide proton. Care need to be taken in limiting the DMSO.d_6 addition to less than 10–15 percent of total solvent volume, as excess would compete with the intramolecular hydrogen bonded protons and disrupt the peptide structure.

3.1.2. *Temperature coefficient*

This method of determination is useful in case the solute is already dissolved in hydrogen bonding solvents like DMSO.d_6 or D_2O or CD_3OH. In such a case, as shown in figure 7 all exposed amide protons forms intermolecular hydrogen bonds with the solvent molecules. Energy involved in such Hydrogen bond is quite low. Small thermal energy provided by heating the sample, is sufficient to break them. Whereas, intramolecular hydrogen bond formed by the shielded proton are relatively higher in energy and hence need much higher temperature to break them. The distinction is made by recording the change in upfield chemical shifts as a function of temperature. These would be linear curves, slope of which yields temperature coefficient ($d\delta/dT$), which is a measure of hydrogen bond. A $d\delta/dT$ value of < 3 ppb/K is indicative of intramolecular hydrogen bond formation of the shielded protons, whereas $>$ 5ppb/K represents plausible exposed amide proton. Caution should be exercised as too high a temperature may disrupt the peptide structure.

3.1.3. *Deuterium exchange*

Yet another way of delineation of hydrogen bond is by exchange of amide protons by deuterium. The peptide sample may be dissolved as quickly as possible in exchange medium like CD_3OD, and spectra are recorded at different time intervals and watch for the disappearance of exposed amide protons as shown in figure 8. It is better to do such experiment at lower temperatures just to slow down the exchange rate and make measurement possible.

4. Protocol for peptide structure by NMR

So far we discussed the basic parameters required for peptides NMR. The flowchart given in scheme 1 illustrates step-by-step approach for peptide NMR analysis. For peptide analysis ^1H homonuclear 1D and 2D NMR would be quite sufficient. Some hetero-correlation experiments like ^1H–^{13}C and ^1H –^{15}N would always strengthen the analysis. For bigger polypeptides or proteins, 3D and even 4D NMR may be needed in which case it becomes necessary to enrich the sample with ^{13}C an ^{15}N labels. But here we restrict ourselves to small natural abundance peptide samples.

The first step is to obtain a good 1D ^1H spectrum with sharp features. Concentrations of few mM would be ideal. Low concentrations are preferred to avoid aggregation. Conformation exchange

Scheme 1: Flowchart showing steps involved for peptide NMR analysis.

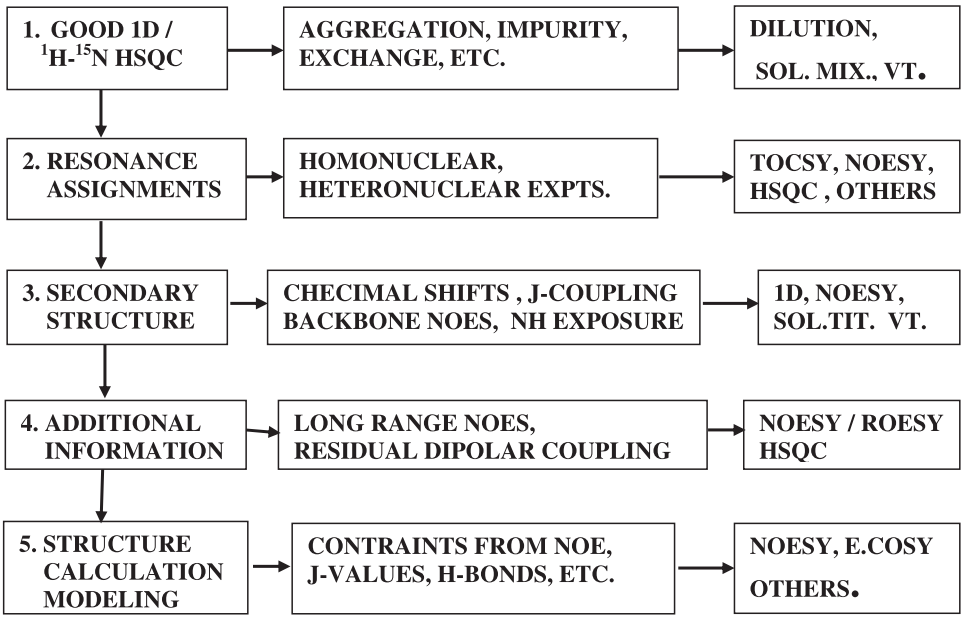

is quite common in peptide sequences and by choosing appropriate temperature, equilibrium could be shifted to one particular conformation. Also temperature influences amide resonance chemical shifts and hence can be used to advantage for obtaining good dispersion. In case of a protein, sharp, well-dispersed ^{1}H-^{15}N spectrum would be the starting point. The next step is the most important step where resonance assignments are done. Here various 2D NMR experiments like DQFC, TOCSY, ROESY, HSQC are used. This has to be foolproof step, and hence the assignments are confirmed from various angles, though it may be repetitive. The third step is the secondary structure assignments, which is mainly done from NOE information and spin-spin coupling (J) values. In the fourth step all possible addition information like long range NOEs, H-bond information, etc. are collected and systematically tabulated. Finally with the help of structure calculating program, which uses these NMR derived parameters, a bunch of structures are calculated. In the following section we describe with an example how we carried out NMR analysis of a designed octapeptide and obtained its structure.

Figure 9: Schematic representation of Boc-Leu-Tyr-Val-^{D}Pro-Gly-Leu-Tyr-Val-OMe (1) in β-hairpin form. Four cross strand hydrogen bonds and Tyr (2) – Tyr(7) aromatic-aromatic interaction are invoked in its stability.

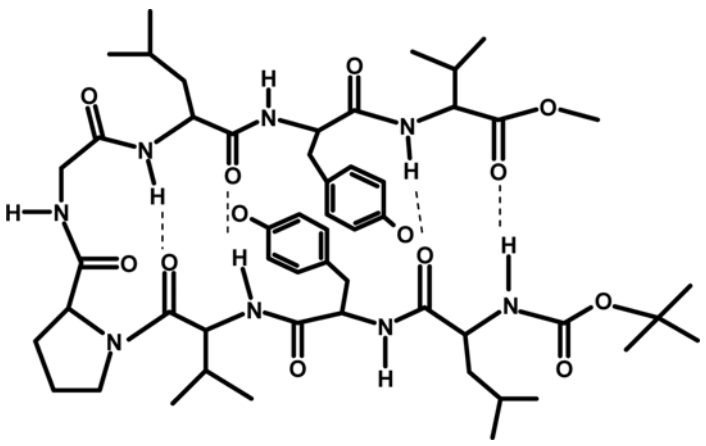

4.1. *An octapeptide as an example*

We consider a case study of an octapeptide Boc-Leu-Tyr-Val-^{D}Pro-Gly-Leu-Tyr-Val-OMe (**1**), which take up a nice β-hairpin conformation as shown in schematic figure 9. The central –(^{D}Pro-Gly)– segment forms a Type II′β-turn. It is flanked on either side by –(Leu-Tyr-Val)– extended segments. The structure is stabilized by 4 intramolecular hydrogen bonds across the strands. Additional stability is provided by Tyr(2) and Tyr(7) aromatic-aromatic stacking interaction [42].

(i) The first step is to get good 1D spectrum with sharp and well-dispersed resonances, which is indicative of a rigid structure. Figure 10, shows a 500 MHz proton 1D spectrum of peptide **1**, in CD_3OH solvent. In addition to good dispersion of

Figure 10: 500 MHz ^{1}H spectrum of peptide 1 in CD_3OH solvent.

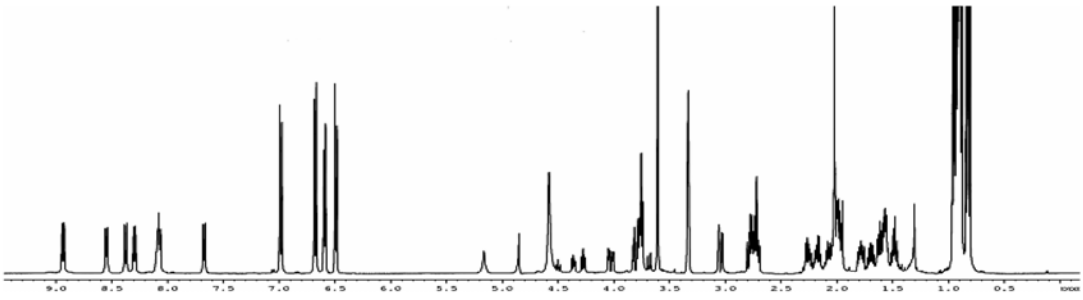

amide resonances, even aromatic resonances from Tyrosine residue are also very well separated. Some of C^α proton resonances close to water resonance could not be seen as they were also suppressed due to strong solvent suppression scheme utilized while recording. However recording the same spectrum in CD_3OD solvent can retrieve them. In such a case we do not need to do solvent suppression, but all amide proton resonances would be lost, as they would undergo exchange with deuterium.

(ii) Sequence specific resonance assignments could easily be carried by 2D – TOCSY and ROESY spectra. This step is the most crucial step, so extreme care has to be taken to make unambiguous assignments. Partial regions of TOCSY and ROESY spectra are shown in figure 11. Residue specific assignment could be done from TOCSY spectrum, as each amino acid would have a unique pattern connecting an amide proton to its backbone C^α proton followed by the remaining sidechain protons. Further with the help of ROESY sequential connectivity either from $d_{NN(i,i+1)}$ or $d_{\alpha N(i,i+1)}$ sequence specific assignments could be done. Chemical shift obtained from these spectra along with $^3J_{NHC^\alpha H}$ spin-spin coupling measured directly from the splitting observed on the amide proton resonances, and temperature coefficients ($d\delta/dT$) obtained from the 1D plots recorded at various temperatures, are tabulated in Table 2.

(iii) Secondary structure information in such small peptides can readily be inferred from the chemical shift spread and $^3J_{NHC^\alpha H}$ spin – spin coupling constant tabulated in Table 2. As mentioned before, the amide- and C^α-proton

Table 2: Tabulation of Chemical shift for peptide (1) along with $^3J_{NHC^\alpha H}$ and Temperature coefficient ($d\delta/d$T) values for amide protons.

Residue	Chemical shift (ppm)					$^3J_{NHC^\alpha H}$ (Hz)	$d\delta/d$T (ppb /K)
	NH	C^αH	C^βH	C^γH	Others		
Leu (1)	7.68	4.61	1.56 1.48	1.47	$C^\delta H_3$:0.90 0.85	8.3	−2.46
Tyr (2)	8.32	5.19	3.04 2.75	–	C^δH: 6.98 C^ϵH: 6.67	9.1	−8.08
Val (3)	8.95	4.50	2.06	0.91 0.90	–	9.4	−4.96
^{D}Pro(4)	–	4.36	1.97	2.25 2.17	$C^\delta H_2$: 3.74	–	–
Gly (5)	8.12	4.02 3.80	–	–	–	–	−9.09
Leu (6)	8.08	4.69	1.77 1.61	1.70	$C^\delta H_3$:0.95 0.94	8.9	−2.79
Tyr(7)	8.58	4.59	2.77 2.71	–	C^δH: 6.58 C^ϵH: 6.48	8.9	−8.51
Val(8)	8.38	4.26	1.97	0.83 0.81	–	9.5	−2.99

Figure 11: (a) ^{1}H 500 MHz Partial region for TOCSY showing connectivities originating from amide protons (top). Resonances from the two aromatic residues can also be distinguished (bottom). (b) Partial ROESY region showing amide-alpha (top) amide-amide connectivities (bottom).

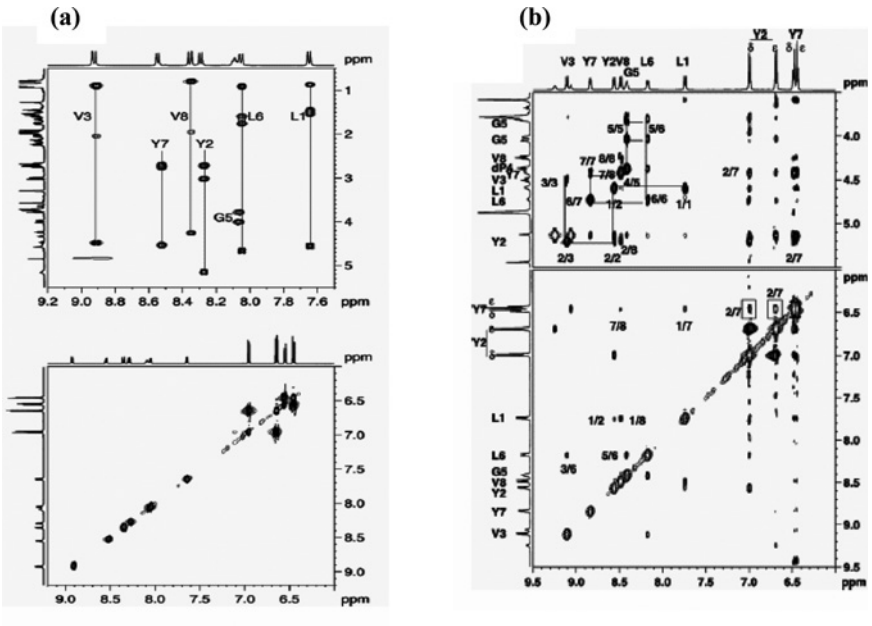

chemical shifts are wide spread and quite down field shifted. These are good indicator of an extended conformation. It is further supported by high $^3J_{NHC^{\alpha}H}$ values (around 9 Hz) for the three residue segment –(Leu-Tyr-Val)– on either side of the –(^{D}Pro-Gly). Synthetic peptide (1) design was based on our earlier work [43]. The goal here was to reinforce the β-hairpin stabilization by additional aromatic interactions across the strands, apart from the regular 4 hydrogen bonds. There is more conclusive evidence for the formation of strands by observation of strong sequential $d_{\alpha N}$ NOEs as shown in figure 11b. Further the hairpin structure is confirm by long range cross strand NOEs such as Leu (1) NH ↔ Val (8) NH, Val (3) NH ↔ Leu (6) NH, Tyr (2) $C^{\alpha}H$ ↔ Val (8) NH, and Tyr (2) $C^{\alpha}H$ ↔ Tyr (7) $C^{\alpha}H$, some of which are shown in figure 11b. Also cross-strand aromatic ring proton NOEs could also be seen, implying the closeness or stacking of aromatic rings.

Presence of 4 hydrogen bonds can be gleaned from the small $d\delta/dT$ values (Table 2) for the amide protons of Leu (1), Val (3), Leu (6), and Val (8), whereas Tyr (2), Gly (5) and Tyr (7) show $d\delta/dT$ value greater than 8ppb /K clearly showing their exposure to solvent which can be seen in the schematic figure 9.

(iv) With the above steps, of which resonance assignment forms the most important step, it is time to cross check and make sure the assignments are absolutely correct, as there is no way we can falter because the future steps take this for granted. Hence, in many cases, resonance assignments are reconfirmed from different angles, such as heteronuclear experiments, etc.

Stereo specific assignments: There are many chemically equivalent protons present in individual amino acid residue such as Glycine $C^{\alpha}H_2$, Leucine $C^{\beta}H_2$, Valine $(C^{\gamma}H_3)_2$, etc. In peptide / protein structure due to a particular fold they usually become inequivalent and show up with different chemical shifts. It is useful to individually assign these resonances stereospecificlly to the appropriate protons, to improve the quality of nmr structure [44]. This can be done by combination of specific J values and the strength of NOE intensities with the nearby protons. For example, consider Newman projection of such an amino acid as shown in the figure 12. The usual three forms guache- (g-), trans (t) and gauche+ (g+) geometry are considered. $^3J_{\alpha\beta}$ coupling could be obtained by an E.COSY experiment [45], so also one can obtain $^3J_{N\beta}$ coupling in case of ^{15}N enriched sample. Typical range of these coupling values are shown at the bottom of the figure 12. Also shown are typical NOE relative strengths. From this combination, it becomes quite easy to stereo specifically assign $\beta 2$ and $\beta 3$ protons.

Figure 12: Three possible rotameric forms (g^- , t, and g^+) of a methylene group as seen through C^α–C^β carbon bond. Corresponding ^3J values and associated relative strength of NOEs are also listed.

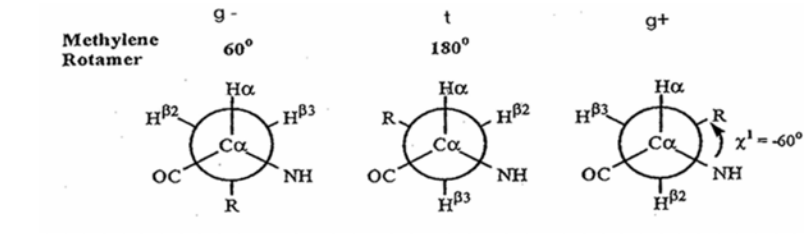

$^3J_{C^\alpha HC^\beta H2}$		low	low	high
$^3J_{C^\alpha HC^\beta H2}$		low	high	low
NOEs	H^α-$H^{\beta2}$	strong	strong	weak
	H^α-$H^{\beta3}$	strong	weak	strong
	NH-$H^{\beta2}$	weak	strong	strong
	NH-$H^{\beta3}$	strong	strong	weak

(v) Having made sure the resonance assignment is foolproof, and obtained some information on secondary structure, it is time to broaden and collect other information at this stage, mainly long range NOEs. It is a good practice to systematically tabulate them. It is even better if they are grouped as sequential $[i, i+1]$, medium range $[i, i+4]$, and long range $[i, > (i+4)]$ NOEs. We add as many NOEs as possible to the list, but make sure it is unambiguously assigned. More the number of NOEs better would be the derived structure. One can also list out some ambiguous NOEs, as the structure calculating software modules has a provision to accommodate such NOEs as well, while refining the structures.

Quantification of NOEs: One way of quantifying the NOE data is to integrate the total volume of a cross peak normalized to a standard distance, which is invariant, such as cross peak across Glycine C^α protons or Proline C^δ protons. Another way is to simply note down the number of contours in a particular cross peak and relate it to the standard. Yet another way is to visually guess the size of the contours and crudely classify them as strong, medium and weak and assign certain range of distance limits [46]. Assuming a practical cutoff of 5 Å as highest observable NOE distance, a weak NOE would be set in the range of 1.9–5.0 Å, a medium NOE would take up 1.9–3.5 Å and a strong NOE could be assigned a range of 1.9–2.2 Å. Note that the lower limit is always set at 1.9 Å which is Vanderwaal limit of internuclear distance, irrespective of the strength of NOE, and only the upper limit which is varied. This is because the dominant dipolar relaxation pathways in solution mediate the NOE. But there are other pathways for relaxation however small, such as chemical shift anisotropy, quadrapolar interaction, etc. So to accommodate these other leakage pathways, the lower limit is always set at the minimum distance of 1.9 Å. A more refined distribution would be by a larger range of selection based on number of contours. However, it is still a range of distances.

Apart from NOE, dihedral angle information obtained through J-coupling network also provides useful constraints for structure calculation. The most common being $^3J_{NHC^\alpha H}$ values which can be fit into the Karplus curve generated by the following equation [46] to obtain ϕ dihedral angle constraint.

$$^3J_{HN\alpha} = 6.4\cos^2\theta - 1.4\cos\theta + 1.9(\theta = |\phi - 60^\circ|) \quad (2)$$

Hydrogen bond information obtained from NMR as mentioned in previous sections adds to the constraints list. NMR can figure out which amide hydrogen is involved in Hydrogen bond, but the corresponding carbonyl Oxygen cannot be unambiguously identified. But from other structural aspects it may not be difficult to predict the plausible carbonyl group, which is involved in a particular hydrogen bond.

Likewise there could be some more NMR parameters like residual dipolar coupling, chemical shift index, etc., from which more constraints can be gathered. More the number of constraints better would be the quality of structure determined.

(vi) Structure calculation: There are couple of NMR structure calculating software available

like CYANA [47], CNS [48], etc., some of them still in public domain which can generate bunch of structures using the NMR generated constraints. They are either distance geometry, or torsion rotation based, having simulated annealing protocols. The inputs to be given for such structure calculations are (i) peptide sequence and (ii) constraints such as interatomic distances as obtained by NOE data, hydrogen bond distance estimates, torsion angles from the spin-spin coupling such as $^{3}J_{NHC^{\alpha}H}$ and others such as residual dipolar couplings etc. Some of these software are more automated which can directly read from the NMR multidimensional spectra, even capable of doing some automatic resonance assignments. The output would consist of the required number of structures along with the various energy contributions and the error list. It is advisable to do only few structures in the beginning and correct the errors, and do the final run with good number of structures, which generally would be around 25–50 structures.

Figure 13 shows a bunch of NMR derived structure using CYANA software on peptide 1. In this analysis, nearly 100 numbers of distance constraints, 8 torsion angles and about 4 pair of hydrogen bond constraints were used. Stereospecific assignment was also done. As a thumb rule, on an average about 10–15 constraints per residue uniformly distributed especially in respect of long range NOE, would provide a decent NMR structure. It may so happen that in some region of peptide sequence, there is good number of constraint and in some other stretch it is poorly distributed. This would show up in the structure as large variation while bunching. Hence rms deviation of these structures is a measure of the quality of structure. In the example of peptide 1 the back bone rmsd was 0.17 ±0.07 Å and mean global heavy atom rmsd of 0.90 ± 0.20 Å. At the terminus the overlap was poor due to lack of good number of constraints at these places.

Figure 13: NMR calculated structure of peptide 1 in methanol. Select 15 best structures are superposed which has an backbone rmsd of 0.17±0.07 Å and mean global heavy atom rmsd of 0.90±0.20 Å.

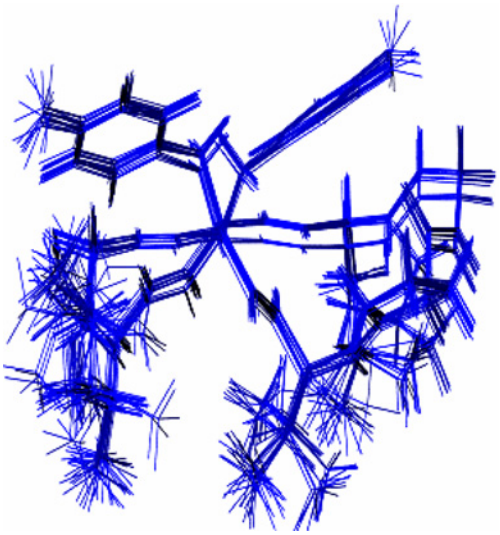

Structure validation: The validation of structures is done by mapping ϕ and ψ dihedral angles on to Ramachandran map. The distribution of dihedral angles of each amino acid on the map over the entire bunch of structures provides analysis quality. Similarly the distribution of side chain dihedral angles such as χ_1 and χ_2 can also be analyzed in terms of variations in the range of gauche-(g-), trans (t), and gauche+ (g+) for each amino acid over the entire bunch of structures. These details sometime help in refining the derived structures.

4.2. *Heteronuclear NMR*

In proteins, heteronuclear multidimensional NMR is routine or essential and hence such proteins are enriched with ^{13}C and ^{15}N isotope labeles through biochemcial pathways. Such isotope labeling in peptides especially synthetic peptides would be very expensive and hence restricted to studies at natural abundance. With current state of the art spectrometers especially with cryo probes, it is quite easy to perform though limited heteronuclear 2D-experiments. The most common being ^{1}H-^{13}C or ^{1}H –^{15}N HSQC [49] experiments. With reasonably good concentration (∼5–10 mM), it is even possible to do 3D-experiments like HSQC-TOCSY and HSQC-NOESY, which could be very useful in resolving overlapping resonances.

4.3. *Analysis of fungal peptides*

Here is a case study of isariins [50], a set of micro heterogeneous cyclohexadepsipeptides isolated from fungus *isaria*. They are very similar peptides differing only in Hydroxyacid methelene chain as shown in figure 14. All of them have similar proton 1D and 2D NMR spectra. Many of the methelene $(CH_2)_n$ protons would overlap around 1.3 ppm, but would spread out in the ^{13}C dimension. A ^{1}H–^{13}C natural abundance heterocorrelation HSQC spectra as shown in figure 14b would indeed help to distinguish the individual peptides.

Similarly natural abundance ^{1}H–^{15}N HSQC spectrum of a ∼ 4KD peptide is shown in figure 15. On 700 MHz spectrometer with cryo probe it took about an hour to record with nearly 2mM concentration. With double this

Figure 14: (a) *Isariins*, cyclic depsipeptides isolated from fungus *isaria*. The five sequences differ only in the Hydroxyacid methelene chain length. (b) 700 MHz partial region of ^{1}H–^{13}C HSQC spectrum showing individual blowup of different isariins differing only in methelene chain length of hydroxyacid.

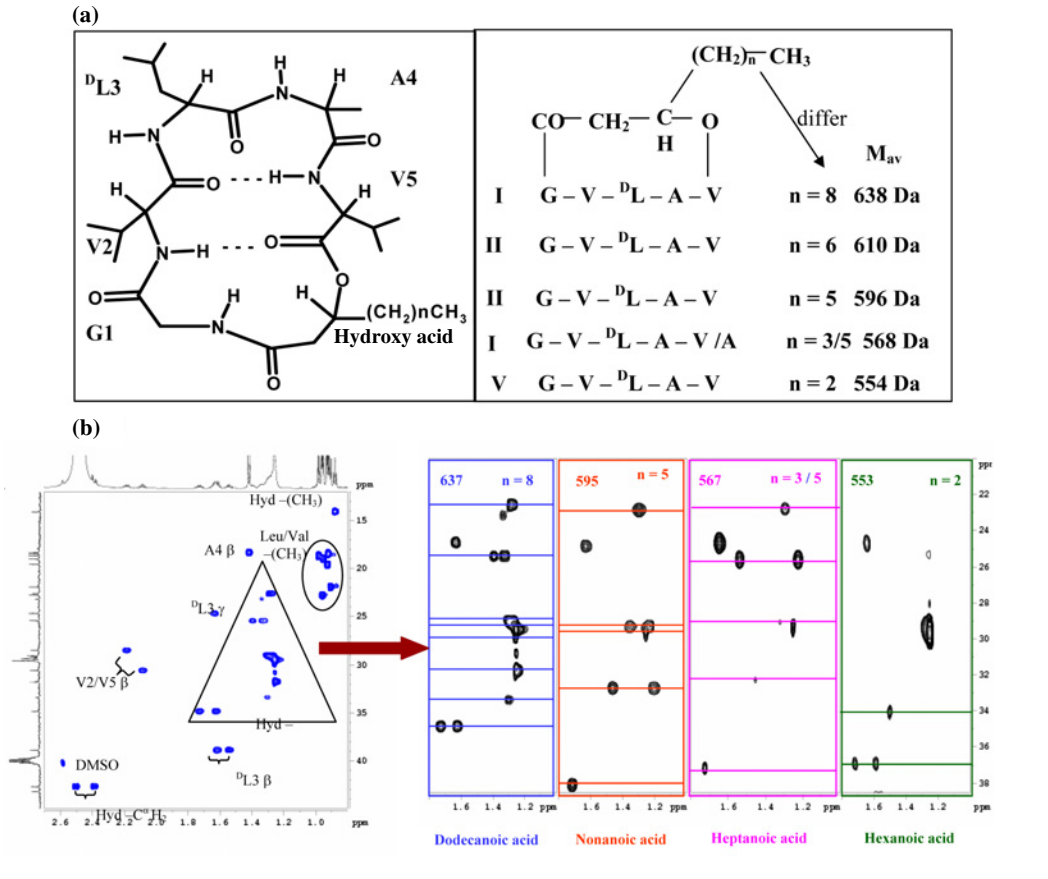

concentration, it would be possible to record 3D HSQC-TOCSY/NOESY in about couple of days time which would provide well resolved constraints for structure calculation, which otherwise may have overlapping resonances in the regular 2D experiments.

4.4. *Multiple conformers*

Peptides are quite flexible due to their small size and hence exists in multiple conformations, which could be undergoing continuous exchange at different rates. NMR has the advantage, that by recording NMR spectra at different temperatures and / or at different spectrometer frequencies, the exchange rates could be monitored. This would give rise to appearance of two, three or more sets of peaks for each resonance at different intensity ratios corresponding to populations of each conformer.

4.4.1. *Cis-trans conformers*

Co-existence of cis-trans conformers in small peptides containing prolines is common [51–53]. Figure 16(a) shows partial ROESY spectrum where two sets of line are observed for the peptide Piv- Pro-Pro-Phe-OMe (2) in $CDCl_3$ solvent. The respective conformers can be diagnostically identified by the $d_{\alpha\alpha}$ and $d_{\alpha\delta}$ NOEs for *cis* and *trans* respectively across the Xxx-Pro segment. Similar information can also be obtained in ^{1}H –^{13}C HSQC where again the peaks are doubled. For peptide (2), a larger $\Delta\delta \sim 10.5$ ppm and smaller $\Delta\delta \sim 2.9$ppm are diagnostic of *cis* and *trans* conformers respectively [30,31], where $\Delta\delta$ is the difference between C^{β}. and C^{γ} carbon chemical shifts.

5. Solid state NMR of peptides

Rich in information content with dipolar and anisotropic interactions, but difficult to unravel, solid state NMR (SSNMR) has taken big strides in current developments [54–57]. Membrane proteins structures, which are difficult to obtain in solution mainly because of poor solubility, are the ideal candidates for solid-state NMR structures [58,59].

Figure 15: Natural abundance 700 MHz ^{1}H–^{15}N HSQC spectrum with ~ 2 mM concentration of a ~4 KD peptide sample in CD_3OH, recorded using cryo probe.

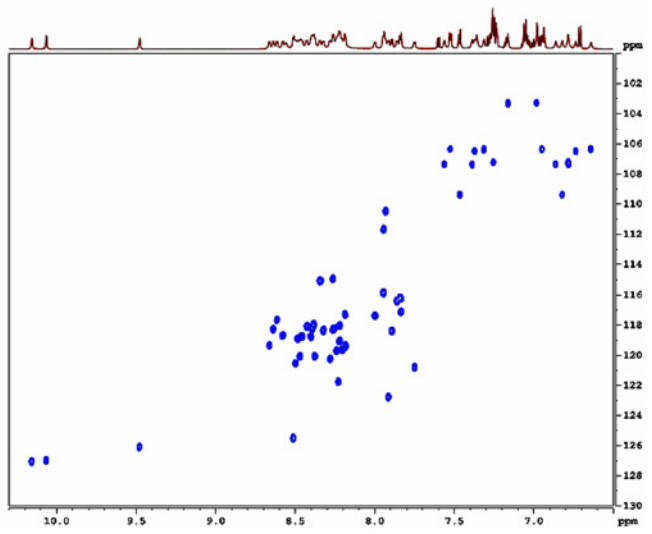

^{1}H spectrum in solid state would be featureless because of difficulty in controlling very strong homogenous interaction. With high magic angle spinning speed touching 70–80KHz and with good decoupling sequences, it is currently possible to get meaningful ^{1}H spectrum with valuable information. However, it is still the rare nuclei like ^{13}C and ^{15}N, which provide structure information for peptides and proteins using multidimensional SSNMR.

5.1. *Peptide solid state NMR at natural abundance*

Good ^{13}C and ^{15}N 1D spectrum using CPMAS (cross polarization magic angle spinning) can easily be done at natural abundance though bit time consuming. Useful information such as polymorphism, chemical shift based structural information can be obtained.

5.2. *Case study on tripeptides containing diproline segments*

Three peptides Piv-^{L}Pro-^{L}Pro-^{L}Phe-OMe (1), Piv-^{D}Pro-^{L}Pro-^{L}Phe-OMe (2) and Piv-^{D}Pro-^{L}Pro-^{L}Phe-NHMe (3) which were well studied by X-ray diffraction and solution NMR [53] was considered for SSNMR at natural abundance [18]. Peptide (1) X-ray structure showed two molecules present in an asymmetric unit and both molecules has *cis* conformation across diproline segment. Whereas the same peptide in solution also showed presence of two conformations but one was in *cis* form and the other was in *trans* [53]. The other similar peptides (2) and (3) showed only *trans* form across the diproline segment. Hence it was interesting to study these peptides by solid state NMR.

^{13}C recording: CPMAS ^{13}C spectra of all three peptides are shown in figure 17. Peptide (2) and (3) had only single set of peaks corresponding to only *trans* form across diproline segment. Almost all resonances for Peptide (1) are doubled. From the chemical shift differences measured for each pair of C^{β}–C^{γ} carbons, $\Delta\delta = 10.3$ and 9.5 ppm respectively [31], it is inferred that both the conformers are in *cis* form unlike in solution where it was *cis* and *trans*.

Figure 16: (a) 500 MHz partial ROESY spectrum of peptide Piv-Pro-Pro-Phe-OMe (2). Two sets of peaks are clearly observed, one set showing pro(1)$C^{\alpha}H$-Pro(2)$C^{\alpha}H$ NOE whereas the other Pro(1)$C^{\alpha}H$ – Pro(2)$C^{\delta}H$ NOE, diagnostic of cis and trans conformation respectively. (b) Similar doubling is shown in ^{1}H-^{13}C HSQC from which ^{13}C chemical shifts diagnostics of cis and trans are obtained which are discussed in the text.

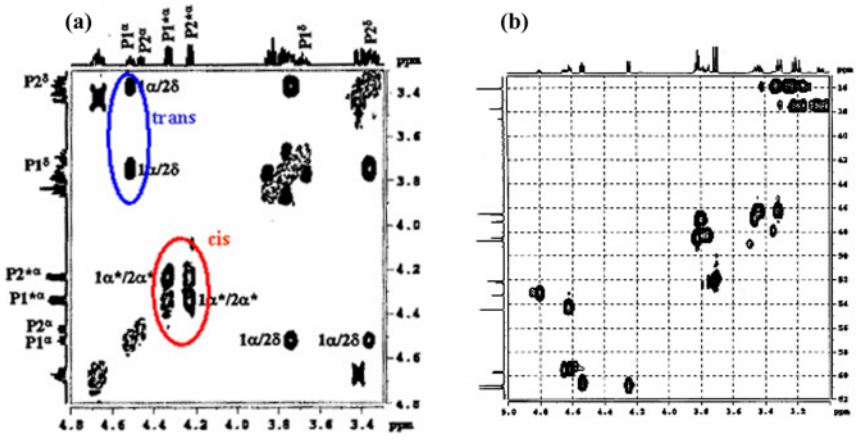

Figure 17: 125MHz CPMAS ^{13}C spectra of (1) Piv-^{L}Pro-^{L}Pro-^{L}Phe-OMe, (2) Piv-^{D}Pro-^{L} Pro-^{L}Phe-OMe, Piv-^{D}Pro-^{L} Pro-^{L}Phe-NHMe. Nearly 30 mg sample packed in rotor and spun at 14 KHz. Doubling of peaks seen in peptide (1). Pro(2) (C^{β}) and Pro(2) (C^{γ}) are marked for peptide (1).

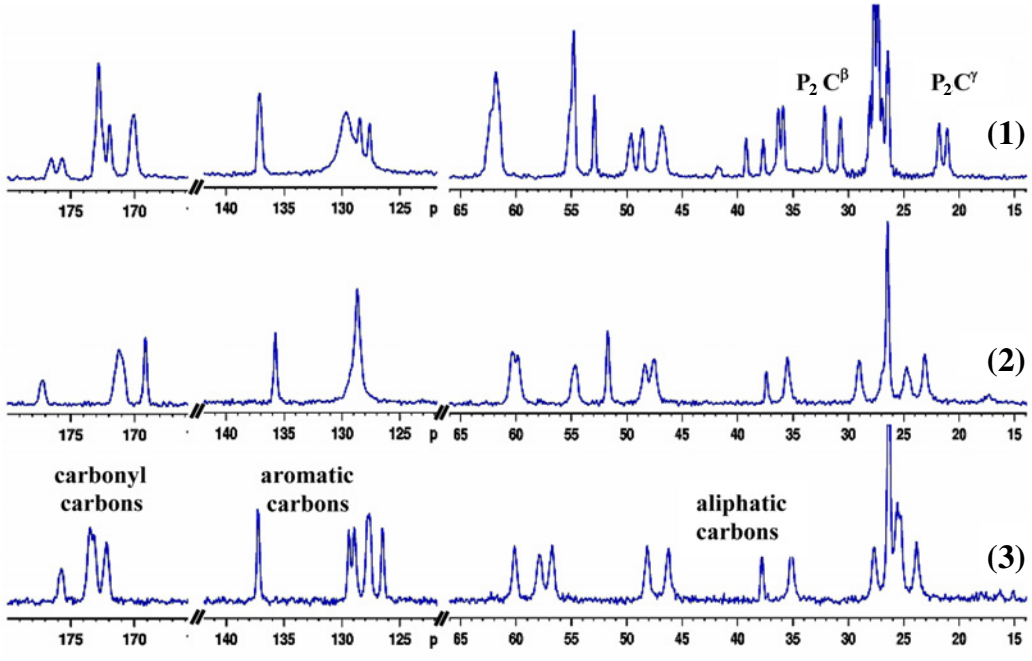

Figure 18: 50 MHz CPMAS ^{15}N spectra of (1) Piv-^{L}Pro-^{L}Pro-^{L}Phe-OMe, (2) Piv-^{D}Pro-^{L} Pro-^{L}Phe-OMe, (3) Piv-^{D}Pro-^{L}Pro-^{L}Phe-NHMe. Rotors spun at 5 KHz. Peptide (1) shows doubling of resonances.

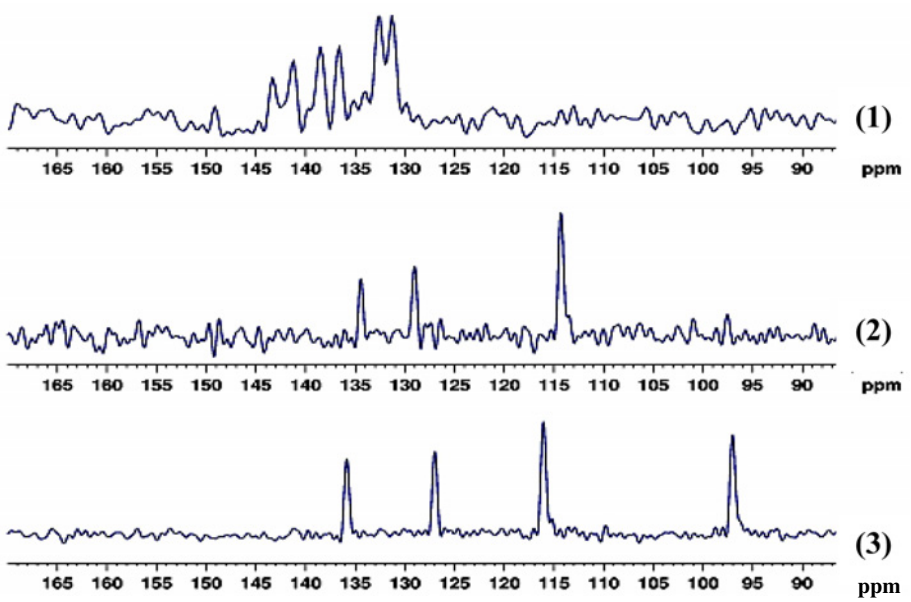

Figure 19: Peptide (3) Piv-^{D}Pro-^{L}PRo-^{L}Phe-NHMe, ^{1}H-^{13}C HETCOR recorded on 500 MHz solid state spectrometer. ^{1}H chemical shift could be obtained from such correlation. Schematic consecutive β-turns suggested for the peptide (3) is shown on the right.

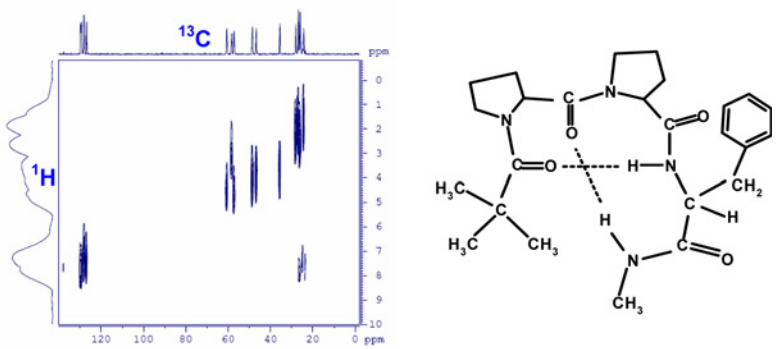

^{15}N recording: Similar information could also be obtained from CPMAS ^{15}N spectrum as shown in figure 18. Here again peptide (2) and (3) showed only one set of resonances, whereas, for peptide (1), all three ^{15}N resonances are doubled. Interesting feature in ^{15}N spectrum was the observation of proline nitrogen as well with reduced intensity which is expected because of absence of directly attached proton. We also see the corresponding nitrogen resonance downfield shifted. In solution such direct observation of Proline nitrogen is quite difficult.

(^{1}H–^{13}C)-Hetcor: Though it is very difficult to get ^{1}H spectrum as described in above paragraph, we could indirectly measure ^{1}H chemical shifts from the natural abundance recording of ^{1}H-^{13}C heterocorrection spectrum as shown in figure 19. Comparison of SSNMR ^{1}H chemical shifts obtained matched with the solution chemical shifts, but for ^{D}Pro(1) C$^{\alpha}$H which was upfield shifted by nearly 1.1 ppm. This is probably because of aromatic ring orientation, which could be eclipsing the said proton. More detailed structural information could be obtained by performing advanced SSNMR techniques such as Separated Local Field Spectroscopy [60] and Proton Encoded local Field spectroscopy [61], which can provide medium and long range dipolar coupling. Such experiments works well with labeled systems. The real challenge lies in obtained such information at natural abundance [62].

6. Conclusions

NMR with its multi-dimensions has become a very powerful tool for peptide analysis. Sensitivity problem has been overcome to a great extent especially with the introduction of cryogenic probes. With further development in the horizon, like Dynamic Nuclear polarization (DNP) (5), it would be a thing of the past. It is now possible to record NMR in micromolar concentration. Natural abundance ^{13}C and ^{15}N experiments have become quite common. Multiple conformers, which are common in peptides, could be analysis independently or simultaneously by monitoring the experimental conditions. Current advances in Solid State NMR, provided yet another additional tool. It would form a nice bridge between the solution and single crystal x-ray structures.

Received 21 January 2010; accepted 16 February 2010.

References

1. Morris. G. A. Magn. Reson. Chem. 24, 371–403, 1986.
2. Methods in Enzymol. Part A & B: Nuclear Magnetic Resonance of Biological Macromolecules, Vol. 338 & 339, 2001. 394. Eds. Thomas, J. L., Volker, D, and Uli, S.
3. Encyclopedia in Nuclear Magnetic Resonance, Vol. 1–9, Eds. Grant. D. M., Harris, R. K. 1995, 2002.
4. Morris. G. A., and Freeman. R. J. Am. Chem. Soc. 101, 760–762, 1979.
5. Barnes, A. B., Paepe. G. D., Van der Wel, P. C. A., Hu, K. N., Joo, C, G., Bajaj, V. S., Jurkauskas, M. L. M., Sirigiri, J. R., Herzfeld, J., Temkin, R. J., and Griffin, R. G. Appl. Magn. Reson. 34, 237–263, 2008.
6. Shrot, Y., Frydman. L. J. Am. Chem. Soc. 125, 11385–11396, 2003.
7. Atreya. H. S., and Szyperski, T. Proc. Natl. Acad. Sci. USA. 101, 9642–9647, 2004.
8. Kupce, E., Freeman, R. J. Am. Chem. Soc. 126, 6429–6440, 2004.
9. Hiller, S., Fiorito, F., Wuthrich. K and Wider. G. Proc. Natl. Acad. Sci. USA., 102, 10876–10881, 2005.
10. Mcdermott. A. E. Annu. Rev. Biophys. 38, 385–403, 2009
11. Karle, I. L. Acc. Chem. Res. 32, 693–701, 1999.
12. R. Rai, S. Aravinda, K. Kanagarajadurai, S. Raghothama, N. Shamala, and P. Balaram. *J. Am. Chem. Soc.* 128, 7916–7928, 2006.
13. Mcdermott, A. E., Curr. Opin. Struct. Biol. 14, 554–561, 2004.
14. Hughes, C.E., Baldus, M. Annu. Rep. NMR Spectrosc. 55, 121–158, 2005.

15. Tycko, R., Methods in Enzymology, Part C, 413, 103–122, 2006.
16. NMR Spectroscopy of Biological Solids; Ed. Ramamoorthy, A. Taylor & Francis: New York, 2006.
17. Harper. J.K., Strohmeier, M, Grant, D.M J. Magn. Reson. 189, 20–31, 2007.
18. S. Jayanthi, S. Bhaswati Chatterjee, Raghothama.S. *Biopolymers,* 91, 851–860, 2009.
19. Shen. Y, Lango, O., Delaglio. F., Rossi, P., Aramini, J. M., Liu. G., Eletsky. A., Wu. Y., Singarapu. K. K., Lemak, A., Ignatchenko, A., Arrowswmith, C. H., Szyperski, T., Montelione, G. T., Baker, D., Bax, A. Proc. Natl. Acad. Sci, USA, 105, 4685–4690, 2008.
20. Cavelli, A., Salvatella, X., Dobson, C.M., Vendruscolo, M., Proc. Natl. Acad. Sci, USA, 104, 9615–9620, 2007.
21. Kohlhoff, K. J., Robustelli, P., Cavalli, A, Salvatella, X., Vendruscolo, M. J. Am. Chem. Soc. 131, 13894–13895, 2009.
22. Proteins: Structures and Molecular Properties Thomas. E. Creighton, Freeman and Co. 1984.
23. Biochemistry: The molecular basis of cell structure and function. 2nd edition, 1978, Albert L. Lehninger. Worth publishers, New York.
24. Lavinthal. C J.Chim.Phys. 65, 44–45, 1968.
25. Zwanzig. R., Szabo, A., and Bagchi, B. Proc. Natl. Acad. Sci. USA., 89, 20–22, 1992.
26. Ramakrishnan, C. Resonance, pp48–56, Oct. 2001.
27. Ramachandran, G.N. and Sasisekharan. V. Adv. Protein Chem. 23, 283–438. 1969.
28. Wishart, D.S., Sykes, B.D., and Richards, F.M. *J. Mol. Biol.* 222, 311–333, 1991.
29. D.S. Wishart, and B.D. Sykes Methods in Enzymology, 239, 363–392, 1994.
30. Richarz. R., Wuthrich, K. Biopolymers, 17, 2133–2141, 1978.
31. Schubert, M., Labudde, D., Oschkinat, H., Schmieder, P.J. Biomol NMR 23, 149–154, 2002.
32. Karplus, M., J. Chem. Phys., 30, 11–15, 1959.
33. Bystrov. V. F., Progr. Nucl. Magn. Reson. Spectros., 10, 41–82, 1976.
34. Pardi, A., Billeter, M. and Wurthrich, K. J. Mol. Biol. 741–751, 1984.
35. Noggle, J. H., Schirmer, R. E., The Nuclear Overhauser Effect, Academic Press, New york, 1971.
36. Neuhaus. D.G. Williamson, M. P., The Nuclear Overhauser Effect in Structural and Conformational Analysis, 2nd Edition, VCH, New York, 2000.
37. Anilkumar, Ermst, Wagner, G., Ernst, R.R. and Wuthrich, K, Biochem. Biophys. Res. Comm. 96, 1156–1163, 1980.
38. Wuthrich, K. J. biol.chem. 265, 22059–22062, 1990.
39. Bothner-By, A.A., Stephens, R.L., Lee, J., Warren, C.D., Jeanloz, R.W. J. Am. Chem. Soc. 106, 811–813, 1984.
40. Bax, A., Davis, D.G. J. Magn. Reson. 63, 207–213, 1985.
41. Davis, D.G., and Bax, A. J. Magn. Reson., 64, 533–535, 1985.
42. NMR Analysis of Aromatic Interactions in Designed Peptide β-Hairpins. R. Mahalakshmi, S. Raghothama, P.Balaram. *J. Am. Chem. Soc*, 128, 1125–1138, 2006.
43. A designed β-hairpin peptide. Satish K Awasthi, S. Raghothama and P. Balaram. *Biochem. Biophys. Res. Comm*., 216, 375, 1995.
44. Protein NMR Techniques (Methods in Molecular Biology) Ed: Reid, D.G., Humana press, New Jersey. 1997.
45. Griesinger, C., Sorenson,O.W., Ernst, R.R., J. Magn. Reson. 75, 474–492, 1987.
46. NMR of Proteins and Nucleic Acids; Wuthrich, K. Wiley: New York, 1986
47. Guntert, P., Mumenthaler, C., Wuthrich, K. J. Mol. Biol., 273, 283–298, 1997.
48. Brunger, A.T., Adams, P.D., Clore, G.M., Delano, W.L., Gros, P., Grosse-Kunstleve, R.W., Jiang, J.S., Kuszewski, J., Nilges, M., Pannu, N.S., Read, R.J., Rice, L.M., Simonson,T., and Warren, G.L. Acta Cryst. D54, 905–921, 1998.
49. Bodenhausen, G., and Ruben, D.J. Chem. Phys. Letters, 69, 185–189, 1980.
50. Sabareesh , R.S. Ranganayaki, S. Raghothama, M.P. Bopanna, Hema Balaram, M.C. Srinivasan and P. Balaram. *J. Natural Products* , 70, 715–729, 2007.
51. Debnath Pal and Pinaki Chakrabarti. J. *Mol.Biol.,* 294, 271–288, 1999.
52. R. Rai, S. Aravinda, K. Kanagarajadurai, S. Raghothama, N. Shamala, P. Balaram. *J. Am. Chem. Soc.* 128, 7916–7928, 2006.
53. B. Chatterjee, I.Saha, S. Raghothama, S. Aravinda, R Rai, N. Shamala, P.Balaram. *Chem. Eur. J.* 14, 6192–6284, 2008.
54. Tycko, R. Ann. Rev. Phys. Chem. 52, 575–606, 2001.
55. Brown, S.P. and Spiess, H.W. Chem. Rev. 101, 4125–4156, 2001.
56. Luca,S.; Heise, H., Baldus, M. Chem. Res. 36, 858–865, 2003.
57. Lee, D.K., Ramamoorthy, A. J. Phys. Chem. B , 103, 271–275, 1999.
58. DeGroot, H.J.M. Curr. Opin. Struct. Biol. 593–600, 2000.
59. Opella, S.J. Nature Struct. Biol. 4 suppl. 845–848, 1997.
60. Hester, R.K.,Ackerman, J.L., Neff.B., Waugh, J.S. Phys. Rev.Lett. 36, 1081–1083, 1976.
61. Schmidt-Rohr, K., Nanz, D., Emsley, L., Pines, A. J. Phys. Chem. 98, 6668–6670, 1994.
62. Yao, X.L., Schmidt-Rohr, K., Hong, M., J. Magn. Reson. 149, 139–143, 2001.

Dr. Raghothama obtained his M.S. degree from Purdue University, USA in the year 1990 and Ph.D from I.I.Sc., Bangalore, India, in the year 1998. He did his post doctoral fellowship at University of Sheffield, U.K during 1998–2000. He is a member of National Academy of Sciences, Allahabad. Currently he holds Principal Research Scientist position at NMR Research centre, IISc. His main research area is in applications of solution and solid state NMR spectroscopic technique to biomolecules.